Application of laser-arc hybrid welding of steel for low temperature service

Ivan Bunaziv[a],*, Odd M. Akselsen[a,b], Jan Frostevarg[c], Alexander F.H. Kaplan[c]

[a] *Norwegian University of Science and Technology, Department of Mechanical and Industrial Engineering, Richard Birkelands vei 2B, NO-7491 Trondheim, Norway*
[b] *SINTEF Industry, P.O. Box 4760 Sluppen, NO-7465 Trondheim, Norway*
[c] *Luleå University of Technology, Department of Engineering Sciences and Mathematics, SE-97187 Luleå, Sweden*

* Corresponding author: ivan.bunaziv@ntnu.no

Abstract

Laser-arc hybrid welding (LAHW) is more often used in shipbuilding and oil and gas industries in recent years. Its popularity arises due to many advantages compared to conventional arc welding processes. The laser beam source is used to achieve much higher penetration depths. By adding filler wire to the process area, by means of an arc source, the mechanical properties can be improved, e.g. higher toughness at low temperatures. Therefore, LAHW is a perspective process for low temperature service. Applicability of LAHW is under concern due to process stability and mechanical properties related to heterogeneous filler wire distribution through the whole weld metal in deep and narrow joints. This can cause reduced mechanical properties in the weld root as well as problems with solidification cracking. The fast cooling rate in the root provides hard and brittle microconstituents lowering toughness at low temperatures. Numerical simulations and experimental observations showed that an increase in heat input from the laser beam is an effective way to reduce the cooling rate, such as also possible by applying preheating.

Keywords: laser beam; hybrid welding; microstructure; toughness; numerical simulation

1. Introduction

The oil and gas, shipbuilding, and pipeline industries frequently utilise thick steel products made from high strength low alloy (HSLA) steel due to the excellent mechanical properties. These steels contain low carbon content for improved weldability. Joining such products by conventional arc welding methods usually requires many passes (multi-pass), which is very time consuming. Due to this, they are ineffective providing low productivity, and reheating of the coarse-grained heat affected zones (CGHAZ) generates martensite-austenite (M-A) islands that is very detrimental for

toughness [1, 2] at low temperature. By application of highly concentrated welding sources such as laser beam welding (LBW) providing higher penetration depths, the number of passes can be reduced to a minimum [3]. The comparison between the two cases is shown in **Fig. 1**. High penetration depth is achieved when high power laser beam works in a keyhole mode, the drilled vapour capillary, which melts the surrounding material. This requires high power density (> 1.5 MW/cm2), focused in a small spot of ~300-800 µm in diameter, to cause boiling and subsequently vaporization of the material. A trapped laser beam inside the keyhole is absorbed, Fresnel absorption

[4-10], by a molten metal of keyhole wall and multiple reflections travel deep generating high penetration depths. This creates a recoil, or ablation, pressure [11] in order to sustain the keyhole opening.

Recently, 1 µm ytterbium fibre laser sources became available at high powers up to 100 kW [12] providing a very high potential in application for joining thick sections [13]. In addition, LBW provides much higher productivity and reduces overall welding operation costs significantly due to higher penetration depth. Another advantage of LBW is the reduced heat input providing much less distortions [14, 15] and lower residual stresses. Residual stresses in welded joints can have a dramatic effect on its integrity, toughness, at low temperatures since they can exceed the yield strength of the base metal inevitably leading to the failure. However, only limited work was done [16, 17] due to difficulties in accurate measurements of residual stresses in welded joints of thick plates.

Laser-arc hybrid welding (LAHW) is a combination of an electric arc with LBW as illustrated in **Fig. 2**. In the case of gas metal arc welding (GMAW), a solid, or flux/metal cored (tubular) filler wire can be used. Tubular wires can further improve the productivity due to higher deposition rate of the filler wire since they have higher electrical resistance causing increased melting efficiency. Moreover, through the addition of alloying elements, the weld microstructure can be better controlled.

In recent years, various researchers achieved good toughness at low temperatures by implementing LAHW technology. Webster et al. [18] applied CO_2 laser-GMAW hybrid welding for 12-25 mm mild steel with single-pass joining within a wide range of welding speeds (0.8-1.2 m/min) and air gaps (0-3 mm). Solid wire was used and Charpy V-notch values > 40 J at -40ºC were achieved. A 20 mm thick HSLA steel was joined by 7.5 kW fibre laser-GMAW hybrid welding with double-sided welding technique by Akselsen et al. [19]. The toughness was > 27 J at -40ºC, in a wide range of welding speeds (0.5-2.0 m/min) and application of solid wire. Gook et al. [20] utilised metal cored wire in joining 20 mm (X80) and 23.4 mm (X100) thick HSLA steel with 14 mm root face for hybrid welding and filling passes made by GMAW, and achieved remarkable toughness of > 60 J at -60ºC. The use of solid wire provided lower toughness. In recent work [21], it was shown that excellent toughness can be achieved (> 45 J at -50ºC) in a wide range of process parameters by using metal cored wire for thick HSLA steel.

An alternative method is multi-pass LBW with filler wire and narrow gap (~3-5 mm). Ultra-narrow gap (1.2 mm) is also possible to utilise [22] for reduction of filler wire and enhance the overall productivity. However, these methods tend to be slow [23-25] and are also susceptible to porosity, cracking and possible lack of sidewall fusion [26, 27].

The paper discusses the application of deep penetration LAHW in joining thick HSLA plates. The effect of important process parameters on the quality of joints are presented. The effect of preheating and dual-beam techniques as alternative solutions is studied based on finite element analysis (FEA). Materials and equipment used in experiments with process parameters are described in detail in previously published work [21, 28-30].
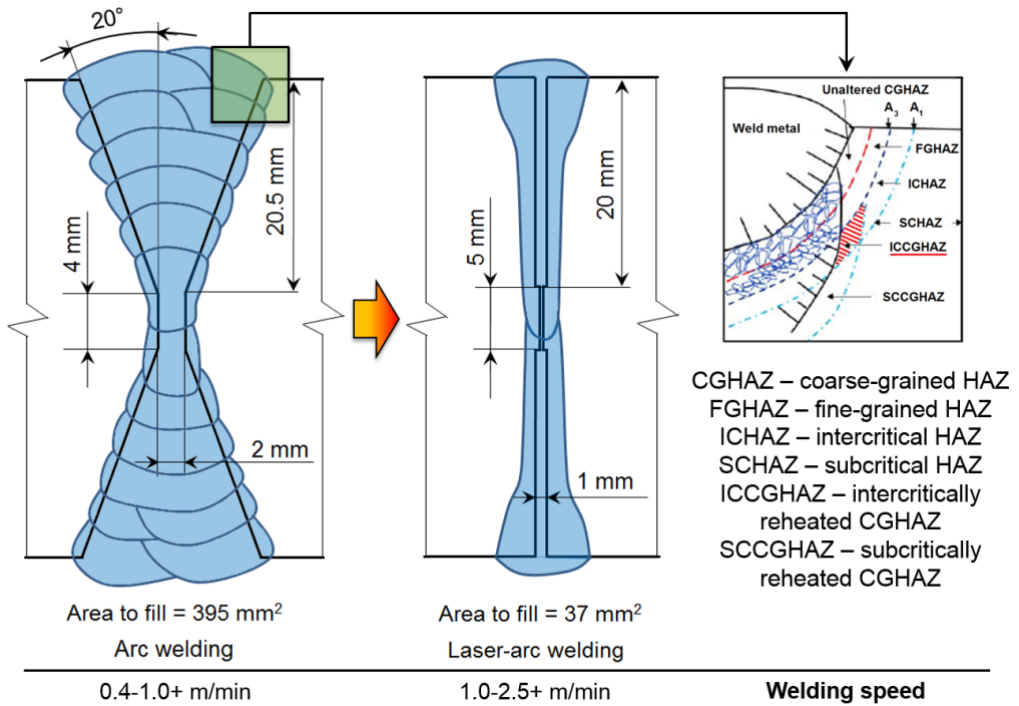
Fig. 1. Multi-pass arc welding versus deep penetration LAHW. Where for arc welding groove preparation geometry is based according to ISO 9692-1, and for LAHW is non-standard based on previous experiments [30].
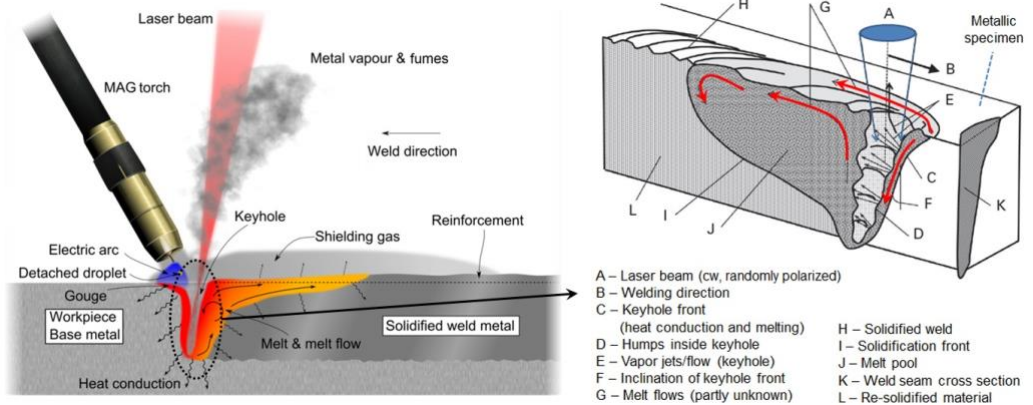

Fig. 2. Physics of laser-arc hybrid welding process. [31, 32]

2. Problems and solutions of deep penetration LAHW joints

Despite the many advantages of deep penetration LAHW, there are also some disadvantages. By combining two sources, the number of welding parameters is vastly increased. Moreover, since they interact with each other [28, 33-44], the optimisation of the process can be extremely complex. Optimisation of the parameters increases process stability, which may eliminate welding defects (e.g. porosity). These can significantly affect the mechanical properties of the welds, specifically the toughness [45] since they may act to initiate brittle fracture. Solidification cracking is also a very common problem due to high depth-to-width ratio in deep penetration welding, which under the prevailing conditions can occur due to weld centreline segregation of impurities and residual tensile stresses [19, 30, 46, 47]. From previous work [30] it was noted that most of the produced LAHW joints had solidification cracks in the root centreline. There was no direct link established to any welding parameter, meaning that it was most likely attributed to high depth-to-width ratio including fairly high strength of the steel used (> 520 MPa), which has more tendency for cracking compared to mild steels [48].

2.1. Filler wire mixing

An important factor is the filler wire delivery, or transportation, to the root or excess dilution of base metal, which may strongly influence the low temperature toughness. This is due to how well the filler wire is homogeneously mixed, or distributed, with base metal throughout the whole weld depth as shown in **Fig. 3**. This problem is not significant when thinner plates are welded and toughness requirements are low, e.g. 27 J at -20ºC. However, when process parameters are not optimised it can appear in thinner plates as well, e.g. 7 mm thick plates [49]. Therefore, this problem is not studied it in detail by the welding community. In welding of thick plates with very high toughness requirements, filler wire distribution is extremely important since it can cause very low mechanical properties in the root zone. Insufficient wire supply to the root may prevent required alloying elements, non-metallic inclusions (NMIs), and hence, acicular ferrite (AF) nucleation causing hard and brittle microstructural constituents such as bainite and lath martensite. Hard microstructures are also mainly attributed to faster cooling rate in the root and will be discussed later.

To quantify how much filler wire that is delivered to the root is a complex task due to a similar chemical composition between the base metal and the wire. In some cases a discoloration can be visible [49] and the mixed/unmixed zone can be identified. Another option is to use different chemical composition wire, e.g. stainless steel, where filler wire distribution can be easily identified by contrast discoloration [21, 50]. In previous work [21, 29], the amount of filler wire delivered was judged by amount of formed AF and hardness values. These are reasonable factors since there is an abrupt hardness increase followed by absence of filler wire providing significantly lower amount of AF.
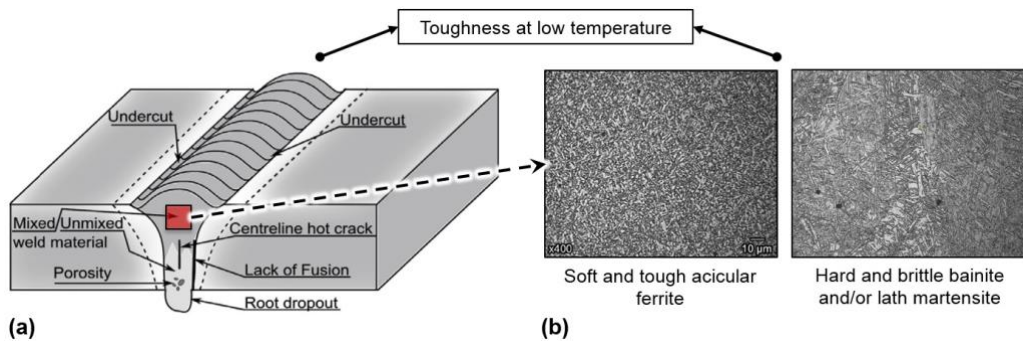
Fig. 3. Two fundamental factors affecting toughness in LAHW of HSLA steels: (a) weld defects [31] and (b) microstructures.

The increase of homogeneity of deep penetrated welds requires optimized process parameters [21, 51], but can also be achieved by using a cut wire placed in the groove prior to welding [29, 52]. By the latter technique, more AF can be found in the root. However, previous work [29] has demonstrated that AF formation is prevented at fast cooling rates (the cooling time between 800 and 500°C, $\Delta t_{8/5}$, was less than 2 s). Thus, a high fraction of NMIs was inactive. As a result, the homogeneity of welds with the cut wire technique has certain limitations. To be able to utilize this technique, and hence provide higher AF fraction at very fast cooling rates, new wires need to be developed. The application of cut wire will be discussed later in more detail.

2.2. Microstructure evolution

The microstructure in low alloy steels has a strong effect on toughness in the weld metal and HAZ. Various microstructural constituents can be formed such as AF, polygonal ferrite (PF), grain boundary ferrite (GBF), Widmanstätten ferrite (WF), bainite (upper, lower), and lath martensite.

It is generally accepted that AF is the most desirable microstructure due to its interlocking morphology of the ferritic plates with high misorientation angles (> 15º) and small grain size (< 3 µm) [53-59]. These are

the main reasons for its excellent fracture toughness. Moreover, AF is also the only constituent that promotes both toughness and strength in combination. Higher AF fraction is more advantageous based on Akselsen and Grong [60], where increase of AF volume fraction from 25% to 75%, increased the toughness by ~40% (at -60ºC), depending on the strength class of the steel. At rapid cooling rates, AF can change its morphology and resemble intragranular AF/WF plates (idiomorphic), which is also frequently surrounded by a hard matrix (bainite, martensite), rather than the fine-grained AF microstructure. In HAZ, AF is not normally found due to the much lower fraction and larger sized NMIs. [53, 56]

PF, or equiaxed ferrite, has low toughness due to larger grain size despite of its softness due to low carbon content. PF is mostly present in weld metal and fine-grained HAZ. [53]

GBF, or allotriomorphic ferrite, has lower toughness due to its very large grain (veins) and favourable crack propagation conditions. It is mostly presents in weld metal. [53, 61]

WF due to its specific orientation, providing low misorientation angles, results in low toughness. WF can be found both in weld metal and HAZ. [53]

Concerning hard microstructures, the lower bainite is somewhat effective in

fracture crack arrestment due to higher misorientation angles of ferritic plates. When compared with upper bainite, which has parallel ferritic plates with aligned M-A films, lower bainite may contain smaller M-A or cementite precipitation within ferritic plates. At very slow cooling rates of CGHAZ, granular bainite is achieved, in low carbon steels, providing low toughness due to low misorientation angles and blocky M-A [62]. Untempered lath martensite has high hardness (within range of ~320-380 HV) and low misorientation angles of blocks and sub-units (laths), and may therefore cause low toughness. Coarse upper bainite and lath martensite are frequently the dominant microstructures found in CGHAZ due to fast cooling rates. [53, 63-65]

2.3. Cooling rate

Due to high penetration depth of the keyhole in LAHW, the distribution of cooling rate is not equal through the whole depth. It significantly increases towards the root of the joint [29], especially when partial penetration welds are made, e.g. double-sided welding. This can be related to the fact that narrower weld pool in the root has considerably smaller volume and temperature decreases much faster. Numerical simulations have shown that substantial variations in the cooling rate along the weld depth (plate thickness direction) can be achieved in high depth-to-width geometrical ratio welds [29, 66].

Measurements of the cooling rate in the weld metal is challenging since the placement of the thermocouples in the root area is inconvenient. A viable option is the ejection of the thermocouple into the fused weld metal (harpooning technique) [67]. However, measurement of the cooling rate in HAZ is rather simple due to easy placement and peak temperature is much lower with no risk in damaging the thermocouple. Turichin et al. [68] measured the cooling rate in the HAZ at the root side and it can be less than 1.0 s depending on the heat input from the laser.

The FEA was used to calculate distribution of the cooling rate from the centreline of weld metal towards the base metal. A detailed modelling procedure can be found elsewhere [29]. One of the selected welds has the following characteristics: leading arc position, 5 mm laser-arc interdistance, 0.4 mm air gap, 0.8 m/min welding speed of the heat sources, 15 kW laser beam power, 4.0 kW arc power (current = 189 A and voltage = 21.4 V). Resulting penetration depth is 20 mm, as measured as partial penetration in 45 mm thick plates. The simulated weld is shown in **Fig. 4** and several points were chosen to represent the cooling rate in different zones for the upper and the root zones. Note that the FGHAZ also includes ICHAZ and SCHAZ since they are very narrow in deep penetration welding and have smaller grains than base metal. According to the results, the cooling rate is almost constant for positions from the weld centreline towards the base metal (BM). The results are consistent with Yang and DebRoy [69] where the simulated and experimental values of the weld metal centreline and the HAZ are nearly the same. As a result, it can be stated that the cooling rate can be measurement based on HAZ values near the weld metal.
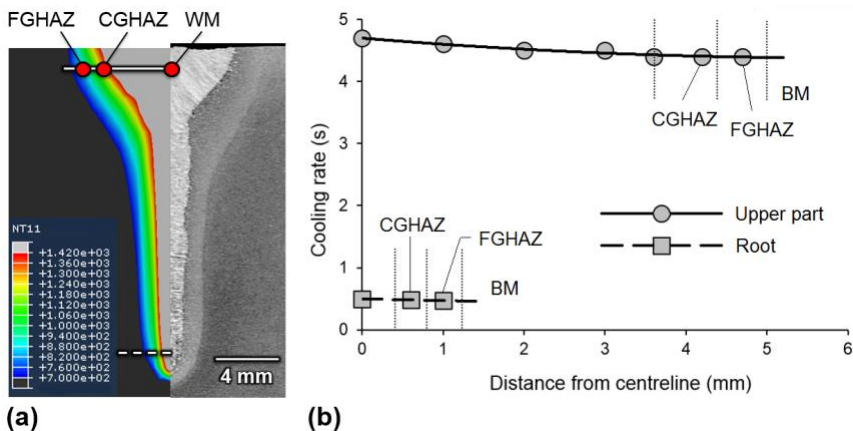
Fig. 4. (a) Simulated welded joint by FEA and (b) distribution of cooling rates in deep penetration LAHW.

To suppress high hardness in the weld metal connected with undesirable microstructure providing low toughness, reduction of the cooling rate can be accomplished by several approaches:

- Increase of the heat input from the heat sources;
- Application of dual-beam laser technique;
- Preheating before or during welding.

Another solution is an increase amount of the deposited passes at expense of productivity, which can be considered as a technical solution. However, the filling passes should be done by arc welding methods as reported in [3, 20, 70]. Otherwise, it requires using large bevelling angles with decrease of productivity and increase of overall costs. Otherwise, making root passes with very low air gap opening is technically impossible.

By using numerical simulations it is possible to predict the resulting microstructure in the coarse grained HAZ by correlating thermal histories to a continuous cooling transformation (CCT) diagram [16]. For the weld metal, the situation is more complex due to the use of filler wire.

However, CCT diagram can also be made for weld metals, but requires more intricate prediction methods [53, 54, 71, 72].

2.3.1. Increase of heat input from laser beam

An increase in heat input is effective in supressing hardness in the root of weld [21] due to slower cooling rate. However, it may generate larger grains in the CGHAZ, which is harmful to toughness [73, 74]. At slower cooling rate, Wang et al. [62] indeed demonstrated low toughness due to the formation of large upper bainite grains containing blocky M-A islands in combination with low misorientation angles between bainite packets. Therefore, lower heat input is preferable for HAZ in spite of the harder microstructures since it provides smaller grains which is more effective in supressing fracture crack propagation [73].

An increase in heat input from the laser beam can be done by reducing welding speed or by increasing laser power. A decrease in welding speed reduces productivity. In order to maintain high productivity, a more powerful laser is needed, and hence, higher cost of investments. The application of higher laser power may require better cooling of the optics to maintain stable processing for a

prolonged production time. An increase of laser power and reduction in welding speed are both have certain limitations, since when maximum penetration depth is reached there is no a reasonable factor for its increase except of specific factors, e.g. reducing root humping defect problem [75] for single pass welding. However, this is not a factor for the double-sided configuration.

In order to increase the heat input, and hence, the weld width with control of penetration depth, a larger spot diameter can be applied, or alternatively change the focal plane position (FPP). Larger spot diameter provides lower penetration depths [50, 76-78] due to lower intensity on the surface. Moreover, Matsumoto et al. [79] demonstrated that larger focused spot diameter, with higher Rayleigh length or focus depth, can provide more stable processing and better quality of the joints in term of porosity. In addition, Schaefer et al. [80] demonstrated that changes in FPP affected clearly the melt flow. This may, in turn, have impact on process stability and weld quality.

2.3.2. Dual-beam technique

The dual-beam, or twin-spot or multi-spot, technique is a possible alternative for thick steel section welding. Up to date, it has not been used extensively due to its complexity [81-83] and high costs of the laser beam sources. According to Xie [84], the hardness of welds was reduced due to slower cooling rate, and weld centreline solidification cracking was not found. In addition, porosity and spattering were suppressed due to more stable vapour plume. Hardness reduction was also achieved in welding of advanced strength steels [85, 86]. The martensite was partly tempered by the second laser beam. However, the second laser beam had similar power as the first beam, and hence, it increased width of the HAZ due to higher heat input. Therefore, distortions and residual stresses are increased. Since LBW and LAHW have inherently significantly lower heat input compared to arc welding, such an increase is probably acceptable.

The simulation results of the dual-beam technique are presented in **Fig. 5**. By using a second laser beam with the same parameters as the first beam, and a laser-to-laser distance of 5 mm, the cooling rate can be reduced by ~280% (from 0.5 s to 1.4 s) in the root. It is related to weld metal width increase, providing larger molten metal volume to cool down. In addition, grain coarsening of the austenite may occur in the CGHAZ, which can be harmful to toughness [62, 73, 74, 87]. However, larger grains are more favourable for AF formation [53, 88, 89], especially when welded steel has specific chemical composition [90-92]. By varying the laser-to-laser distance and the total laser beam power, including other specific parameters (e.g. pulsing characteristics and/or focal spot diameter), a better control over thermal cycles can be achieved. Moreover, by using FEA the optimum parameters can be found avoiding expensive experimental trials. Still, the use of dual laser beams needs further investigation to understand its impact on mechanical properties and fracture toughness. Indications are that the heat input from the second laser beam must be carefully controlled.

Presumably, the beam parameters of the second laser beam (e.g. beam parameter product, BPP) with smaller focused spot diameter should be preferable to reach higher penetration depth with minimum heat input in the upper part of the weld.
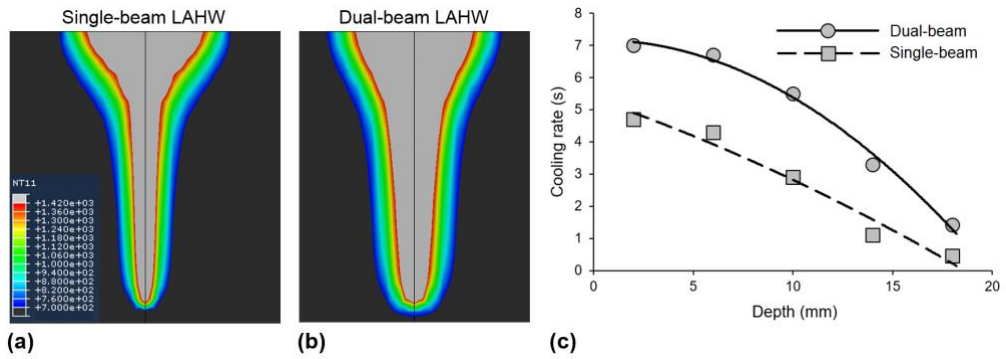
Fig. 5. Effect of dual-beam LAHW on weld geometry and cooling rate.

2.3.3. Preheating

The cooling rate can be extended by preheating before or during welding at relatively high temperature (say > 100°C). The preheating can be local or global. However, preheating can be an expensive procedure and should be used only if strictly required. For local preheating induction heating is a viable option and proven to be effective for thin plates **[93, 94]** and for thicknesses up to 20 mm **[95]**.

The effectiveness of preheating depends on temperature and thickness of the specimen according to Yurioka et al. **[96]**. Based on their work, the effectiveness of preheating temperature decreases at > 130°C regardless heat input, especially for thinner plates. The FEA results is presented **Fig. 7** with selected preheating temperatures of 130°C and 250°C. A global preheating at 130°C had a minor effect on cooling rate in the root, it was reduced only by 40% (from 0.5 s to 0.7 s), which is not sufficient to obtain softer microstructure for better toughness. Preheating at 250°C extended the cooling rate by ~240% (from 0.5 s to 1.2 s). For the highest preheating temperature there is an increase in weld metal and HAZ width. It is also expected that this preheating may reduce hardness. Accordingly, it is suggested to apply ≥ 200°C preheating for partial deep penetration process. Alternatively, post weld heat treatment (PWHT) can be applied, but it is not desired from a production and cost effectiveness standpoint.
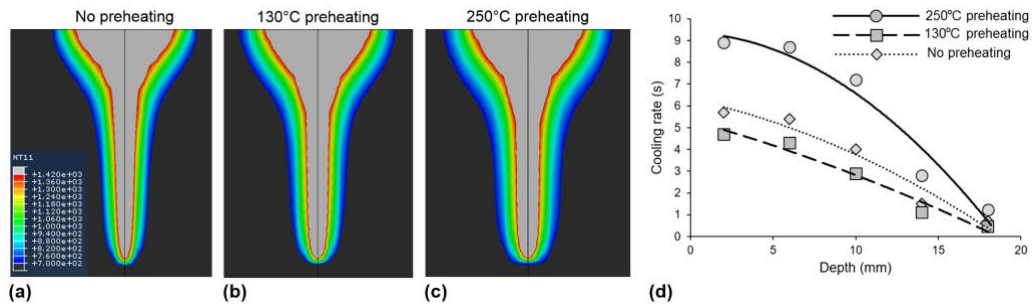

Fig. 6. Effect of preheating temperature on cooling rate.

3. Effect of process parameters on quality of joints

LAHW contains a substantial number of process parameters. Here, the effect of each them is discussed concerning the quality of joints. Since the parameters interact with each other, they are interdependent, and some experiments were made with changing more than one variable at the time. Therefore, the discussion provided interpreting the interdependency factor.

3.1. Effect of welding speed

The welding speed is a primary parameter that affects the process stability and subsequently the quality of joints [28, 79, 97-102]. It also influences the penetration depth. A reduction in welding speed provides deeper penetration [103], but the relationship is non-linear, specifically at lower welding speed.

Recent results [28] have shown that welding speed higher than 0.6 m/min in the CMT+P arc mode becomes unstable, producing a wire chopping destabilisation phenomena. By striking the keyhole opening area, this may generate weld defects such as porosity. Spattering was also observed in these experimental trials when the chopped wire hit the surface area close to or into the weld pool, which significantly disturbed the melt flow. An increase of wire feed rate (or current) can eliminate this problem since arc rooting is enhanced [99, 104]. However, a conventional pulsed arc mode can also create such destabilisation.

Based on the conducted experiments [21], the welds having the faster welding speeds (1.0-1.2 m/min) provided lower AF fractions in the root, even with large air gaps (0.8-1.0 mm) and moderate heat input from the laser beam (0.8-0.9 kJ/mm). As a potential result, the melt flow is unfavourable, and the supplied wire stays in the upper part of the weld pool. Therefore, not much fused filler is transported to the root to provide higher amount of AF. The effect of welding speed on the AF fraction in the root (average AF fraction at 75% and 95% depth) is shown in **Fig. 7** by the one-way analysis of variance (ANOVA) regression method which is described elsewhere [30]. Note that only welds having similar penetration depths (17-21 mm) and 4-5 mm laser-arc interdistance [21] are included. According to the results, the AF fraction is reduced with an increase in travel speed regardless of other process parameters (arc mode, wire feed rate, arc position, air gap, and groove preparation geometry). Such trend can also be related to the stability of the melt hydrodynamics. At lower travel speed it is more stable based on experimental observation of deep penetration LBW conducted by Fabbro [97]. Kawahito et al. [105] showed that the keyhole diameter decreases with increasing welding speed; so does the absorption of the laser beam [8]. Presumably, the smaller keyhole diameter has higher probability to be overflown by the added filler wire and has lower transportation capability of the filler wire.
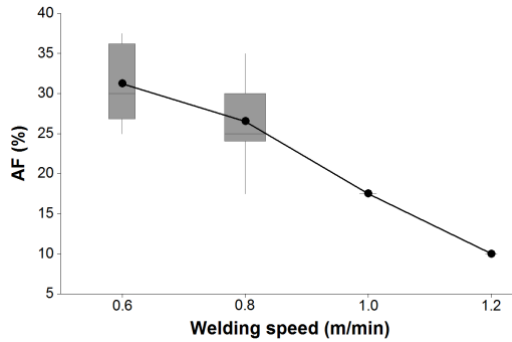
Fig. 7. Effect of welding speed on AF fraction in root area.

3.2. Effect of air gap

The presence of an air gap between welded plates increases the AF fraction in the root part in deep penetration LAHW [21]. As a consequence, the hardness level is also reduced. This may be related to more favourable melt flow, which transports the filler wire more effectively to the deeper parts of the joint. However, at this point cannot be proven since it requires the use of X-ray radiography and tracing particles in order to study melt flow during processing. Application of a simpler method as the use of stainless steel wire is not viable due to high expenses to reproduce welds.

By increasing the air gap less base metal is melted, and therefore lower dilution is achieved. Lower dilution is positive for more favourable microstructure evolution since re-melted base metal cannot provide high AF fraction due to lower amount of NMIs. However, it also depends on the cooling rate. In previous work [29], it was shown that in spite of large amount of NMIs, a low fraction of AF is achieved since most NMIs remained inactive at fast cooling rates.

In addition, air gap is very effective in providing higher penetration depths [18, 30], e.g. increasing productivity. This is mainly due to the fact that less volume of base metal needed to be melted and potentially enhanced multiple reflections inside the air gap [104] causing higher beam absorption and more efficient melting. However, the wire feed rate must be increased when the air gap is extended. The associated increase in current can be harmful since it causes higher heat input (wider HAZ and coarser grains in the upper part of the weld) and the extra molten filler material can overflow the keyhole, especially for shorter laser-arc interdistances and leading arc arrangements [28, 33, 104]. Moreover, the stability of the keyhole dynamics inside larger air gap and the flow of molten material around it is under concern [36]. Under these conditions, large pores, or root humping in single pass welding may occur [75].

3.3. Effect of arc power and arc mode

The effect of arc heat input, or filler wire feed rate, on the cooling rate in the root area is very low since the heat dissipates in the upper part of the joint as stated previously [21]. The FEA results are given in **Fig. 8**. It is clearly shown that the cooling rate did not change in the root. Moreover, an increase of arc power can destabilise keyhole dynamics and cause weld imperfections (spatter, porosity), as shown by previous work [28, 30]. The destabilised keyhole can be related to an increase of the arc plasma drag force and the arc pressure [106, 107], since both factors directly depends on the current, pushing molten metal towards the keyhole. This is a concern for both the arc position (trailing or leading) especially when the laser-arc interdistance is short (~1-5 mm).

11

Another reason is that the metal overflow at an increased filler wire feed rate may cause collapse of the keyhole. As a result, the effect of arc power on keyhole stability must be studied in detail in LAHW.

The CMT+P arc mode has improved stability in terms of droplet transfer [28]. The wire feed rate of this technique is limited, up to 10 m/min. Thick plate welding with large air gaps requires large amount of filler wire which may not be provided by CMT+P. On the other hand, this arc more can provide much lower heat input (by ~40-120%), depending on the wire feed rate [30]. Unfortunately, this did not lead to an improvement of the Charpy V-notch and CTOD results [21]. This can relate to the fact that the tested samples were extracted from the root of the joint where the arc power has very limited effect, see **Fig. 8**.

Frostevarg [49] found that the CMT+P arc mode provided better weld metal mixing with increased air gap compared to pulsed or standard arc mode, presumably due to more favourable melt flow. However, relatively thin plates (7 mm thick carbon steel) were used for this task. No relation to the arc mode was identified in the case of deep penetration LAHW [21].

When compared to CMT+P, the conventional pulsed arc mode is potentially more beneficial. Here, higher frequency of droplets are hitting the weld pool having higher momentum (smaller in size) with increased velocities [108] possessing much higher kinetic energy. This may, in turn, force the melt down towards the root. Although, the melt of keyhole and its interaction with the arc melt might have a more significant effect on filler wire transportation to the root. Moreover, conventional pulsed arc has higher currents, and therefore, can be more harmful for the keyhole stability leading to some compromise in LAHW making it a very intricate process. Unfortunately, no further study was done on the effect of arc mode on weld metal mixing capability.
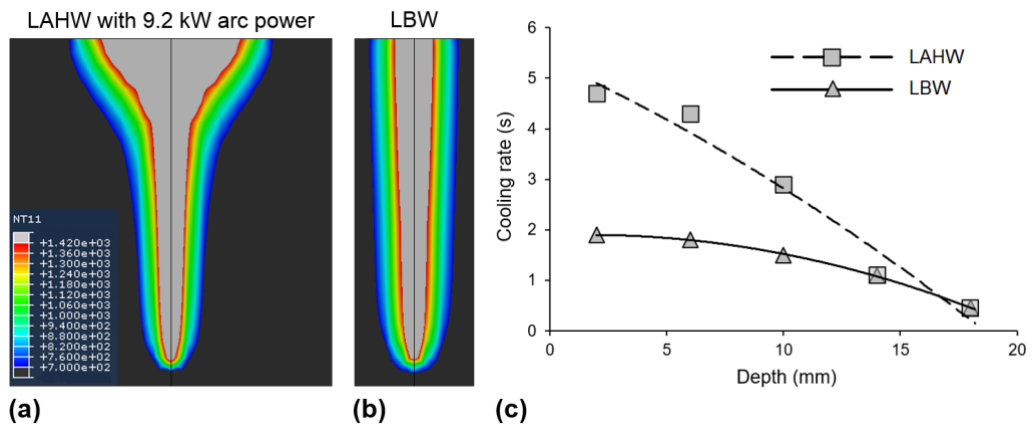

Fig. 8. Effect of arc heat input on cooling rate.

3.4. Effect of arc position and laser-arc interdistance

The quality of the joints in LAHW significantly depends on the laser-arc interdistance and arc position [15, 21, 28, 30, 33, 36, 38, 40, 50, 104, 109-121] since they have a strong interdependency. Both process parameters affect melt flow dynamics and penetration depth, as discussed elsewhere [30].

Based on the experimental observations [28], a leading arc position has the droplet flight trajectory deflected towards the keyhole. This can provide severe porosity within short laser-arc interdistances. The CMT+P arc mode is more preferable since the trajectory deflection is weaker compared to the pulsed arc mode. An increased wire feed rate can raise the probability of keyhole collapse. Whereas at longer laser-arc distances, the processing is stable and wire feed rate can be increased when it is required, e.g. at higher welding speed. Shorter laser-arc interdistance is safer to use in trailing arc position setup since the droplet flight trajectory is deflected from the keyhole.

Application of shorter laser-arc interdistances can provide favourable melt flow resulting in higher homogeneity in the weld metal. However, in leading arc case longer laser-arc interdistance can be more beneficial for filler wire mixing due to more favourable melt flows [21]. Longer laser-arc interdistance in trailing arc setup is not suitable since the melt flows mainly to the rear part of the weld pool in this case. It is unlikely that the melt is delivered to the root area by keyhole melt flow [50], and weld pools can be completely separated at too long laser-arc interdistance [15]. Tsukamoto et al. [122] showed that trailing arc is more preferable due to inward melt flow to the root.

Concerning the air gap, laser-arc interdistance and arc position, which are all interdependent, their combined effects on process behaviour has not been clearly identified due to lack of experiments. It has not either been studied in detail by other researchers. The maximum applicable air gap, the bridgeability, has not been identified. A physical model was proposed by Petring et al. [123], but the model does not reflect any dependency on laser-arc interdistance and arc position. It is more affected by other process and physical parameters (e.g. material density, surface tension and gravitational force).

The summary of results and optimisation strategy is represented in **Fig. 9**, where high level of process parameters (on the left) and low process parameters (on the right) are separated. It presents that higher level of process parameters are more advisable for welding of thick section regardless arc position. However, too high level can be inappropriate and cause unstable processing.

Due to very high complexity of LAHW and vast process parameters, there is still a large window for process improvement by optimisation. This is a complex due to their high interdependency, e.g. laser-arc interdistance, arc position, welding speed, air gap and arc power (wire feed rate). High speed imaging can provide better understanding of the process. However, it is restricted to the surface of the weld pool whereas melt flow and stability in deeper parts remain unknown. Therefore, X-ray filmography [103, 124, 125] with tracing particles can provide better understanding of the process. Another solution is to apply a *sandwich* method [126-128], where the steel is combined with transparent material, and that allows to study keyhole behaviour with a conventional optical high speed camera.

In addition, numerical simulation can be calibrated and established for predicting quality of welds for industrial use. Moreover, FEA utilizing computational fluid dynamics (CFD) [37, 81, 82, 129-141] can reduce very expensive testing of LBW/LAHW. There is a high interest in predicting the amount of filler wire transported to the root. More advanced filler wire can be developed for higher AF formation ability at fast cooling rates. Preheating before welding and dual-beam technique can be carried out for assessment

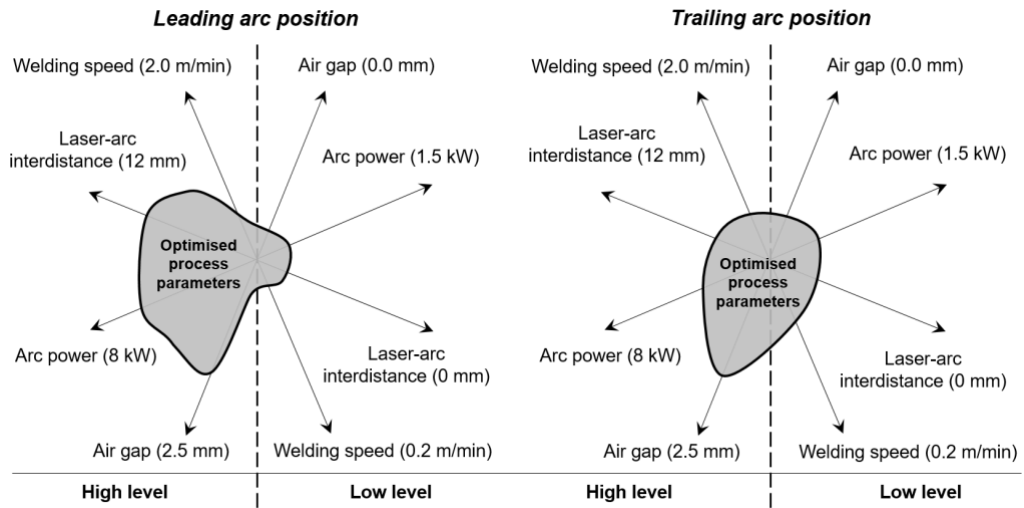of its viability to increase cooling rate in the root and compare it with the provided numerical simulations.

Fig. 9. Optimisation of process parameters in LAHW for thick steel sections.

3.5. Application of preplaced cut wire

Recently, a cut wire was preplaced in the groove before welding to increase weld homogeneity for the deep penetration LAHW [52]. However, no toughness properties were published. Subsequently, cut wire was applied in welding HSLA steel [29], with results showing favourable microstructure evolution with low hardness in the root. Welds produced with the cut wire technique showed lower Charpy V-notch toughness at -50°C when compared to conventional LAHW setup. However, still the toughness was high (74 J) for both the weld metal and the HAZ. CTOD testing revealed rather low toughness values for the cut wire experiments despite the very high number (density) of NMIs due to low base metal dilution. Thus, these inactive NMIs most likely favoured brittle fracture propagation [61], due to bainite formation, even though porosity was not observed in welds made with cut wire. By this method, larger air gaps must be applied due to low packing density. This leads to higher filler wire consumption and higher costs. An alternative to cut wire is to add powder, but this causes a further rise in welding costs. In fact, powders will give better packing density compared to randomly packed filler wire (1-3 mm length) with potentially lower amount of porosity. However, an increased laser power or reduced welding speed must be applied since stacked preplaced cut wires act as a solid. Therefore, heat input is increasing during welding which in turn causes problems with toughness in HAZ, e.g. larger width and coarser grain size. Moreover, the wire must be straight. Therefore, the wire from a spool is unlikely applicable since it has some curvature and additional straightening mechanisms must be adapted.

4. Conclusions

Application of LAHW is a possible solution for welding of thick steel plates with high toughness requirements for low temperature service. However, it requires a sophisticated optimisation of process parameters for suitability due to complexity. The main problems associated with thick section welding are process stability, fast cooling rate in the root and homogeneity of welds, which are all important for appropriate mechanical properties. Since the process offers very high productivity implementation of the process in industry production is considered feasible. According to the numerical simulations, preheating and dual-beam technology can be viable in prolonging cooling rate in the root for hardness decrease. It has been shown that LAHW of thick plates with metal cored wire can produce welds with acceptable toughness at down to -50ºC.

Acknowledgements

References

1.   Akselsen, O.M., J.K. Solberg, and Ø. Grong, *Effects of martensite-austenite (M-A) islands on intercritical heat-affected zone toughness of low carbon microalloyed steels.* Scandinavian Journal of Metallurgy 1988. **17**: p. 194-200.

2.   Akselsen, O.M., Ø. Grong, and J.K. Solberg, *Structure–property relationships in intercritical heat affected zone of low-carbon microalloyed steels.* Materials Science and Technology, 1987. **3**(8): p. 649-655.

3.   Nielsen, S.E., *High Power Laser Hybrid Welding – Challenges and Perspectives.* Physics Procedia, 2015. **78**(Supplement C): p. 24-34.

4.   Kaplan, A.F.H., *Local absorptivity modulation of a 1 μm-laser beam through surface waviness.* Applied Surface Science, 2012. **258**(24): p. 9732-9736.

5.   Kaplan, A.F.H., *Fresnel absorption of 1 μm- and 10 μm-laser beams at the keyhole wall during laser beam welding: Comparison between smooth and wavy surfaces.* Applied Surface Science, 2012. **258**(8): p. 3354-3363.

6.   Kaplan, A.F.H., *Absorption homogenization at wavy melt films by CO2-lasers in contrast to 1 μm-wavelength lasers.* Applied Surface Science, 2015. **328**(0): p. 229-234.

7.   Wang, H., Y. Kawahito, R. Yoshida, Y. Nakashima, and K. Shiokawa, *A model to calculate the laser absorption property of actual surface.* International Journal of Heat and Mass Transfer, 2018. **118**: p. 562-569.

8.   Kaplan, A., *A model of deep penetration laser welding based on calculation of the keyhole profile.* Journal of Physics D: Applied Physics, 1994. **27**(9): p. 1805-1814.

9.   Cheng, Y., X. Jin, S. Li, and L. Zeng, *Fresnel absorption and inverse bremsstrahlung absorption in an actual 3D keyhole during deep penetration CO2 laser welding of aluminum 6016.* Optics & Laser Technology, 2012. **44**(5): p. 1426-1436.

10.   Matsunawa, A., and V. Semak, *The simulation of front keyhole wall dynamics during laser welding.*

Journal of Physics D: Applied Physics, 1997. **30**(5): p. 798.

11. Kaplan, A.F.H., *Local flashing events at the keyhole front in laser welding.* Optics and Lasers in Engineering, 2015. **68**(0): p. 35-41.

12. Shcherbakov, E.A., V.V. Fomin, A.A. Abramov, A.A. Ferin, D.V. Mochalov, and V.P. Gapontsev, *Industrial grade 100 kW power CW fiber laser*, in *Advanced Solid State Lasers*. 2013.

13. Grupp, M., K. Klinker, and S. Cattaneo, *Welding of high thicknesses using a fibre optic laser up to 30 kW.* Welding International, 2011. **27**(2): p. 109-112.

14. Standfuss, J., E. Beyer, B. Brenner, R. Schedewy, D. Dittrich, and R. Strohbach, *Laser-multi-pass-welding of aluminium and steel with sheet thickness above 50mm*, in *34th International Congress on Applications of Lasers & Electro-Optics (ICALEO)*. 2015, LIA: Atlanta, Ga., USA. p. 626-631.

15. Reutzel, E.W., S.M. Kelly, M.J. Sullivan, T.D. Huang, L. Kvidahl, and R.P. Martukanitz, *Hybrid Laser-GMA Welding for Improved Affordability.* Journal of Ship Production, 2008. **24**(2): p. 72-81.

16. Ren, X., S.K. Ås, O.M. Akselsen, and B. Nyhus, *Comparison of Hybrid Laser-arc and Conventional Welding for Arctic Applications*, in *21st International Offshore and Polar Engineering Conference (ISOPE)*. 2011: Maui, Hawaii, USA.

17. Ren, X.B., Z.L. Zhang, and B. Nyhus, *Effect of residual stress on cleavage fracture toughness by using cohesive zone model.* Fatigue & Fracture of Engineering Materials & Structures, 2011. **34**(8): p. 592-603.

18. Webster, S., J.K. Kristensen, and D. Petring, *Joining of thick section steels using hybrid laser welding.* Ironmaking & Steelmaking, 2008. **35**(7): p. 496-504.

19. Akselsen, O.M., G. Wiklund, E. Østby, A. Sørgjerd, and A. Kaplan. *A First Assessment of Laser Hybrid Welding of 420 MPa Steel For Offshore Structure Applications*. in *14th Nordic Laser Materials Processing Conference (NOLAMP)*. 2013. Gothenburg, Sweden.

20. Gook, S., A. Gumenyuk, and M. Rethmeier, *Hybrid laser arc welding of X80 and X120 steel grade.* Science and Technology of Welding and Joining 2014. **19**(1): p. 15-24.

21. Bunaziv, I., O.M. Akselsen, J. Frostevarg, and A.F.H. Kaplan, *Deep penetration fiber laser-arc hybrid welding of thick HSLA steel.* Journal of Materials Processing Technology, 2018. **256**: p. 216-228.

22. Guo, W., L. Li, S. Dong, D. Crowther, and A. Thompson, *Comparison of microstructure and mechanical properties of ultra-narrow gap laser and gas-metal-arc welded S960 high strength steel.* Optics and Lasers in Engineering, 2017. **91**: p. 1-15.

23. Zhang, C., G. Li, M. Gao, and X. Zeng, *Microstructure and Mechanical Properties of Narrow Gap Laser-Arc Hybrid Welded 40 mm Thick Mild Steel.* MDPI (Materials), 2017. **10**(2).

24. Yamazaki, Y., Y. Abe, Y. Hioki, M. Nakatani, A. Kitagawa, and K. Nakata, *Fundamental study of narrow-gap welding with oscillation laser beam.* Welding International, 2016. **30**(9): p. 699-707.

25. Näsström, J., J. Frostevarg, and T. Silver, *Hot-wire Laser Welding of Deep and Wide Gaps.* Physics Procedia, 2015. **78**: p. 247-254.

26. Shi, H., K. Zhang, J. Zheng, and Y. Chen, *Defects inhibition and process optimization for thick plates laser welding with filler wire.*

Journal of Manufacturing Processes, 2017. **26**(Supplement C): p. 425-432.

27. Wu, S., J. Zhang, J. Yang, J. Lu, H. Liao, and X. Wang, *Investigation on microstructure and properties of narrow-gap laser welding on reduced activation ferritic/martensitic steel CLF-1 with a thickness of 35 mm.* Journal of Nuclear Materials, 2018. **503**: p. 66-74.

28. Bunaziv, I., J. Frostevarg, O.M. Akselsen, and A.F.H. Kaplan, *Process stability during fiber laser-arc hybrid welding of thick steel plates.* Optics and Lasers in Engineering, 2018. **102**(Supplement C): p. 34-44.

29. Bunaziv, I., O.M. Akselsen, J. Frostevarg, and A.F.H. Kaplan, *Laser-arc hybrid welding of thick HSLA steel.* Journal of Materials Processing Technology, 2018. **259**: p. 75-87.

30. Bunaziv, I., J. Frostevarg, O.M. Akselsen, and A.F.H. Kaplan, *The penetration efficiency of thick plate laser-arc hybrid welding.* The International Journal of Advanced Manufacturing Technology, 2018. **97**(5): p. 2907-2919.

31. Frostevarg, J., *The Morphology of Laser Arc Hybrid Welds*, in *Department of Engineering Sciences and Mathematics, Product and Production Development*. 2014, Luleå University of Technology: Luleå tekniska universitet, 2014.

32. Katayama, S., *Handbook of Laser Welding Technologies* 2013: Woodhead Publishing

33. Fellman, A., and A. Salminen. *Study of the Phenomena of Fiber Laser-MAG Hybrid Welding*. in *26th International Congress on Applications of Lasers and Electro-Optics (ICALEO)*. 2007. Orlando, Florida, USA: Laser Institute of America.

34. Hu, B., and G. den Ouden, *Laser induced stabilisation of the welding arc.* Science and Technology of Welding and Joining, 2005. **10**(1): p. 76-81.

35. Hu, B., and G. den Ouden, *Synergetic effects of hybrid laser/arc welding.* Science and Technology of Welding and Joining, 2005. **10**(4): p. 427-431.

36. Hayashi, T., S. Katayama, N. Abe, and A. Omori, *High-power CO2 laser-MIG hybrid welding for increased gap tolerance. Hybrid weldability of thick steel plates with a square groove.* Welding International, 2004. **18**(9): p. 692-701.

37. Ribic, B., T.A. Palmer, and T. DebRoy, *Problems and issues in laser-arc hybrid welding.* International Materials Reviews, 2009. **54**(4): p. 223-244.

38. Kutsuna, M., and L. Chen. *Interaction of Both Plasmas in CO2 Laser-MAG Hybrid Welding of Carbon Steel*. in *LAMP 2002: International Congress on Laser Advanced Materials Processing*. 2003. SPIE.

39. Wahba, M., M. Mizutani, and S. Katayama, *Hybrid welding with fiber laser and CO2 gas shielded arc.* Journal of Materials Processing Technology, 2015. **221**(0): p. 146-153.

40. Abe, N., Y. Kunugita, M. Hayashi, and Y. Tsuchitani, *Dynamic Observation of High Speed Laser-Arc Combination Welding of Thick Steel Plates.* Transactions of JWRI, 1997. **26**(2): p. 7-11.

41. Liu, S., F. Zhang, S. Dong, H. Zhang, and F. Liu, *Characteristics analysis of droplet transfer in laser-MAG hybrid welding process.* International Journal of Heat and Mass Transfer, 2018. **121**: p. 805-811.

42. Steen, W.M., *Arc augmented laser processing of materials.* Journal of

Applied Physics, 1980. **51**(11): p. 5636-5641.

43. Olsen, F., *Hybrid laser-arc welding*. 2009: Woodhead Publishing.

44. Turichin, G., E. Valdaytseva, I. Tzibulsky, A. Lopota, and O. Velichko, *Simulation and Technology of Hybrid Welding of Thick Steel Parts with High Power Fiber Laser.* Physics Procedia, 2011. **12, Part A**(0): p. 646-655.

45. You, C.P., and J.F. Knott, *Effects of crack shape on fracture toughness in a high-strength structural steel.* Engineering Fracture Mechanics, 1986. **24**(2): p. 291-305.

46. Wiklund, G., O.M. Akselsen, A.J. Sørgjerd, and A. Kaplan, *Geometrical aspects of hot cracks in laser-arc hybrid welding.* Journal of Laser Application, 2014. **26**.

47. Gebhardt, M.O., A. Gumenyuk, and M. Rethmeier, *Solidification cracking in laser GMA hybrid welding of thick-walled parts.* Science and Technology of Welding and Joining, 2013. **19**(3): p. 209-213.

48. Sokolov, M., A. Salminen, M. Kuznetsov, and I. Tsibulskiy, *Laser welding and weld hardness analysis of thick section S355 structural steel.* Materials & Design, 2011. **32**(10): p. 5127-5131.

49. Frostevarg, J., *Comparison of three different arc modes for laser-arc hybrid welding steel* Journal of Laser Applications, 2016. **28**: p. 022407.

50. Victor, B., B. Nagy, S. Ream, and D. Farson. *High Brightness Hybrid Welding of Steel*. in *28th International Congress on Applications of Lasers and Electro-Optics (ICALEO)*. 2009. Orlando, Florida, USA.

51. Frostevarg, J., A. Kaplan, and J. Lamas, *Comparison of CMT with other arc modes for laser-arc hybrid welding of steel.* Welding in the World, 2014. **58**(5): p. 649-660.

52. Wahba, M., M. Mizutani, and S. Katayama, *Single pass hybrid laser-arc welding of 25 mm thick square groove butt joints.* Materials & Design, 2016. **97**(Supplement C): p. 1-6.

53. Bhadeshia, H.K.D.H., and R.W.K. Honeycombe, *Steels: Microstructure and Properties*. 3rd ed. 2006: Butterworth-Heinemann.

54. Babu, S.S., *The mechanism of acicular ferrite in weld deposits.* Current Opinion in Solid State and Materials Science, 2004. **8**(3): p. 267-278.

55. Díaz-Fuentes, M., A. Iza-Mendia, and I. Gutiérrez, *Analysis of different acicular ferrite microstructures in low-carbon steels by electron backscattered diffraction. Study of their toughness behavior.* Metallurgical and Materials Transactions A, 2003. **34**(11): p. 2505-2516.

56. Ricks, R.A., P.R. Howell, and G.S. Barritte, *The nature of acicular ferrite in HSLA steel weld metals.* Journal of Materials Science, 1982. **17**(3): p. 732-740.

57. Wan, X.L., H.H. Wang, L. Cheng, and K.M. Wu, *The formation mechanisms of interlocked microstructures in low-carbon high-strength steel weld metals.* Materials Characterization, 2012. **67**(Supplement C): p. 41-51.

58. Kim, K.H., J.S. Seo, C. Lee, and H.J. Kim, *Grain Size of Acicular Ferrite in Ferritic Weld Metal.* Welding in the World, 2011. **55**(9): p. 36-40.

59. Yang, J.R., and H.K.D.H. Bhadeshia, *Acicular ferrite transformation in alloy-steel weld metals.* Journal of Materials Science, 1991. **26**(3): p. 839-845.

60. Akselsen, O.M., and Ø. Grong, *Prediction of weld metal Charpy V notch toughness.* Materials Science and Engineering: A, 1992. **159**(2): p. 187–192.

61. Tweed, J.H., and J.F. Knott, *Micromechanisms of failure in C☐Mn weld metals.* Acta Metallurgica, 1987. **35**(7): p. 1401-1414.

62. Wang, X.L., Z.Q. Wang, L.L. Dong, C.J. Shang, X.P. Ma, and S.V. Subramanian, *New insights into the mechanism of cooling rate on the impact toughness of coarse grained heat affected zone from the aspect of variant selection.* Materials Science and Engineering: A, 2017. **704**(Supplement C): p. 448-458.

63. Bhadeshia, H.K.D.H., and J.W. Christian, *Bainite in steels.* Metallurgical Transactions A, 1990. **21**(3): p. 767-797.

64. Bhadeshia, H.K.D.H., *Bainite in Steels: Transformations, Microstructure and Properties*. 2nd ed. 2001: IOM Communications.

65. Bhadeshia, H.K.D.H., *Bainite in Steels: Theory and Practice*. 3rd ed. 2015: Maney Publishing.

66. Tan, W., and Y.C. Shin, *Multi-scale modeling of solidification and microstructure development in laser keyhole welding process for austenitic stainless steel.* Computational Materials Science, 2015. **98**: p. 446-458.

67. Moore, P.L., *Novel method of recording cooling curves during laser & laser/arc hybrid welding*, in *JOM 11*. 2003.

68. Turichin, G., M. Kuznetsov, M. Sokolov, and A. Salminen, *Hybrid Laser Arc Welding of X80 Steel: Influence of Welding Speed and Preheating on the Microstructure and Mechanical Properties.* Physics Procedia, 2015. **78**(Supplement C): p. 35-44.

69. Yang, Z., and T. Debroy, *Modeling macro-and microstructures of Gas-Metal-Arc Welded HSLA-100 steel.* Metallurgical and Materials Transactions B, 1999. **30**(3): p. 483-493.

70. Chen, Y., J. Feng, L. Li, S. Chang, and G. Ma, *Microstructure and mechanical properties of a thick-section high-strength steel welded joint by novel double-sided hybrid fibre laser-arc welding.* Materials Science and Engineering: A, 2013. **582**: p. 284-293.

71. Babu, S.S., and H.K.D.H. Bhadeshia, *Transition from bainite to acicular ferrite in reheated Fe–Cr–C weld deposits.* Materials Science and Technology, 1990. **6**(10): p. 1005–1020.

72. Babu, S.S., and S.A. David, *Inclusion Formation and Microstructure Evolution in Low Alloy Steel Welds.* ISIJ International, 2002. **42**(12): p. 1344-1353.

73. Zhou, Y., T. Jia, X. Zhang, Z. Liu, and R.D.K. Misra, *Microstructure and toughness of the CGHAZ of an offshore platform steel.* Journal of Materials Processing Technology, 2015. **219**(Supplement C): p. 314-320.

74. Lambert-Perlade, A., T. Sturel, A.F. Gourgues, J. Besson, and A. Pineau, *Mechanisms and modeling of cleavage fracture in simulated heat-affected zone microstructures of a high-strength low alloy steel.* Metallurgical and Materials Transactions A, 2004. **35**(3): p. 1039-1053.

75. Frostevarg, J., *Factors affecting weld root morphology in laser keyhole welding.* Optics and Lasers in Engineering, 2018. **101**(Supplement C): p. 89-98.

76. Qin, G.L., Z. Lei, and S.Y. Lin, *Effects of Nd:YAG laser + pulsed MAG arc hybrid welding parameters on its weld shape.* Science and Technology of Welding and Joining, 2007. **12**(1): p. 79-86.

77. Liu, Z., M. Kutsuna, and G. Xu. *Fiber Laser Welding of 780MPa High Strength Steel*. in *25th International Congress on*

Applications of Lasers and Electro-Optics (ICALEO). 2006. Scottsdale, Arizona, USA: Laser Institute of America.

78. Vänskä, M., F. Abt, R. Weber, A. Salminen, and T. Graf, *Effects of Welding Parameters Onto Keyhole Geometry for Partial Penetration Laser Welding.* Physics Procedia, 2013. **41**(0): p. 199-208.

79. Matsumoto, N., Y. Kawahito, K. Nishimotoa, and S. Katayama, *Effects of laser focusing properties on weldability in high-power fiber laser welding of thick high-strength steel plate.* Journal of Laser Applications, 2017. **29**(1): p. 012003.

80. Schaefer, M., S. Kessler, F. Fetzer, and T. Graf, *Influence of the focal position on the melt flow during laser welding of steel.* Journal of Laser Applications, 2017. **29**(1): p. 012010.

81. Chen, X., X. Zhang, S. Pang, R. Hu, and J. Xiao, *Vapor plume oscillation mechanisms in transient keyhole during tandem dual beam fiber laser welding.* Optics and Lasers in Engineering, 2018. **100**: p. 239-247.

82. Pang, S., W. Chen, J. Zhou, and D. Liao, *Self-consistent modeling of keyhole and weld pool dynamics in tandem dual beam laser welding of aluminum alloy.* Journal of Materials Processing Technology, 2015. **217**: p. 131-143.

83. Li, L., H. Xia, G. Ma, and G. Peng, *Flow dynamics during single- and dual-spot laser welding with one common keyhole of 321 stainless steel.* Journal of Materials Processing Technology, 2018. **255**: p. 841-852.

84. Xie, J., *Dual Beam Laser Welding.* Welding Journal, 2002. **81**(10): p. 223-230.

85. Morawiec, M., M. Różański, A. Grajcar, and S. Stano, *Effect of dual beam laser welding on microstructure–property*

relationships of hot-rolled complex phase steel sheets. Archives of Civil and Mechanical Engineering, 2017. **17**(1): p. 145-153.

86. Grajcar, A., M. Morawiec, M. Różański, and S. Stano, *Twin-spot laser welding of advanced high-strength multiphase microstructure steel.* Optics & Laser Technology, 2017. **92**: p. 52-61.

87. Lan, L., X. Kong, C. Qiu, and D. Zhao, *Influence of microstructural aspects on impact toughness of multi-pass submerged arc welded HSLA steel joints.* Materials & Design, 2016. **90**(Supplement C): p. 488-498.

88. Grong, O., *Metallurgical Modelling of Welding*. 1994: Maney Pub.

89. Wan, X.L., K.M. Wu, K.C. Nune, Y. Li, and L. Cheng, *In situ observation of acicular ferrite formation and grain refinement in simulated heat affected zone of high strength low alloy steel.* Science and Technology of Welding and Joining, 2015. **20**(3): p. 254-263.

90. Homma, H., S. Ohkita, S. Matsuda, and K. Yamamoto, *Improvement of HAZ Toughness in HSLA Steel by Introducing Finely Dispersed Ti-Oxide.* Welding Journal, 1987. **66**: p. 301-309.

91. Pan, Y.-T., and J.-L. Lee, *Development of TiOx-bearing steels with superior heat-affected zone toughness* Materials & Design 1994. **15**(6): p. 331-338.

92. Zhang, D., H. Terasaki, and Y.-i. Komizo, *In situ observation of the formation of intragranular acicular ferrite at non-metallic inclusions in C–Mn steel.* Acta Materialia, 2010. **58**(4): p. 1369-1378.

93. Coelho, R.S., M. Corpas, J.A. Moreto, A. Jahn, J. Standfuß, A. Kaysser-Pyzalla, and H. Pinto, *Induction-assisted laser beam welding of a thermomechanically rolled HSLA S500MC steel: A microstructure and residual stress*

assessment. Materials Science and Engineering: A, 2013. **578**(Supplement C): p. 125-133.

94. Jahn, A., M. Krätzsch, and B. Brenner. *Induction assisted laser beam welding of HSLA steel sheets*. in *International Scientific Colloquium Modelling for Electromagnetic Processing*. 2008. Hannover: Univ. Hannover.

95. Lahdo, R., O. Seffer, A. Springer, S. Kaierle, and L. Overmeyer, *GMA-laser Hybrid Welding of High-strength Fine-grain Structural Steel with an Inductive Preheating*. Physics Procedia, 2014. **56**: p. 637-645.

96. Yurioka, H., H. Suzuki, S. Ohshita, and S. Saito, *Determination of Necessary Preheating Temperature in Steel Welding*. Welding Journal, 1983. **62**: p. 147-153.

97. Fabbro, R., *Melt pool and keyhole behaviour analysis for deep penetration laser welding*. Journal of Physics D: Applied Physics, 2010. **43**(44): p. 445501.

98. Fabbro, R., S. Slimani, I. Doudet, F. Coste, and F. Briand, *Experimental study of the dynamical coupling between the induced vapour plume and the melt pool for Nd–Yag CW laser welding*. Journal of Physics D: Applied Physics, 2006. **39**(2): p. 394-400.

99. Tsukamoto, S., T. Sugino, T. Nakamura, and G. Arakane. *Fundamental Study on Welding Phenomena in Pulsed Laser-GMA Hybrid Welding*. in *24th International Congress on Applications of Lasers and Electro-Optics (ICALEO)*. 2005. Miami, Florida, USA: Laser Institute of America.

100. Madison, J.D., and L.K. Aagesen, *Quantitative characterization of porosity in laser welds of stainless steel*. Scripta Materialia, 2012. **67**(9): p. 783-786.

101. Kawahito, Y., M. Mizutani, and S. Katayama, *Elucidation of high-power fibre laser welding phenomena of stainless steel and effect of factors on weld geometry*. Journal of Physics D: Applied Physics, 2007. **40**(19): p. 5854.

102. Panwisawas, C., B. Perumal, R.M. Ward, N. Turner, R.P. Turner, J.W. Brooks, and H.C. Basoalto, *Keyhole formation and thermal fluid flow-induced porosity during laser fusion welding in titanium alloys: Experimental and modelling*. Acta Materialia, 2017. **126**: p. 251-263.

103. Katayama, S., Y. Kawahito, and M. Mizutani, *Elucidation of laser welding phenomena and factors affecting weld penetration and welding defects*. Physics Procedia, 2010. **5, Part B**(0): p. 9-17.

104. Fellman, A., *The effects of some variables on CO2 laser-MAG hybrid welding*. 2008, Lappeenranta University of Technology.

105. Kawahito, Y., N. Matsumoto, Y. Abe, and S. Katayama, *Relationship of laser absorption to keyhole behavior in high power fiber laser welding of stainless steel and aluminum alloy*. Journal of Materials Processing Technology, 2011. **211**(10): p. 1563-1568.

106. Hu, J., and H.L. Tsai, *Heat and mass transfer in gas metal arc welding. Part I: The arc.* International Journal of Heat and Mass Transfer, 2007. **50**(5–6): p. 833-846.

107. Hu, J., and H.L. Tsai, *Heat and mass transfer in gas metal arc welding. Part II: The metal.* International Journal of Heat and Mass Transfer, 2007. **50**(5–6): p. 808-820.

108. Hu, J., and H.L. Tsai, *Metal Transfer and Arc Plasma in Gas Metal Arc Welding*. Journal of Heat Transfer, 2006. **129**(8): p. 1025-1035.

109. Bunaziv, I., O.M. Akselsen, A. Salminen, and A. Unt, *Fiber laser-MIG hybrid welding of 5mm 5083*

aluminum alloy. Journal of Materials Processing Technology, 2016. **233**(Supplement C): p. 107-114.

110. Zhao, L., T. Sugino, G. Arakane, and S. Tsukamoto, *Influence of welding parameters on distribution of wire feeding elements in CO2 laser GMA hybrid welding.* Science and Technology of Welding and Joining, 2009. **14**(5): p. 457-467.

111. Piili, H., A. Salminen, P. Harkko, and J. Lehtinen. *Study of Phenomenon of Fibre-Laser-Mig/Mag-Hybrid-Welding.* in *27th International Congress on Applications of Lasers and Electro-Optics (ICALEO).* 2008. Temecula, California, USA: Laser Institute of America.

112. Naito, Y., and M. Mizutani. *Observation of Keyhole Behavior and Melt Flows during Laser-Arc Hybrid Welding.* in *22th International Congress on Applications of Lasers and Electro-Optics (ICALEO).* 2003. Jacksonville, Florida, USA: Laser Institute of America.

113. Murakami, T., M.-H. Shin, and K. Nakata, *Effect of welding direction on weld bead formation in high power fiber laser and MAG arc hybrid welding.* Transactions of JWRI, 2010. **39**(2): p. 175-177.

114. Huang, L., D. Wu, X. Hua, S. Liu, Z. Jiang, F. Li, H. Wang, and S. Shi, *Effect of the welding direction on the microstructural characterization in fiber laser-GMAW hybrid welding of 5083 aluminum alloy.* Journal of Manufacturing Processes, 2018. **31**: p. 514-522.

115. Ascari, A., A. Fortunato, L. Orazi, and G. Campana, *The influence of process parameters on porosity formation in hybrid LASER-GMA welding of AA6082 aluminum alloy.* Optics & Laser Technology, 2012. **44**(5): p. 1485-1490.

116. Casalino, G., S.L. Campanelli, U. Dal Maso, and A.D. Ludovico, *Arc Leading Versus Laser Leading in the Hybrid Welding of Aluminium Alloy Using a Fiber Laser.* Procedia CIRP, 2013. **12**(0): p. 151-156.

117. Frostevarg, J., and A. Kaplan, *Undercut suppression in laser-arc hybrid welding by melt pool tailoring.* Journal of Laser Applications, 2014. **26**(3).

118. Liu, L.M., S.T. Yuan, and C.B. Li, *Effect of relative location of laser beam and TIG arc in different hybrid welding modes.* Science and Technology of Welding and Joining, 2012. **17**(6): p. 441-446.

119. Liu, L., J. Shi, Z. Hou, and G. Song, *Effect of distance between the heat sources on the molten pool stability and burn-through during the pulse laser-GTA hybrid welding process.* Journal of Manufacturing Processes, 2018. **34**: p. 697-705.

120. Kang, K., Y. Kawahito, M. Gao, and X. Zeng, *Effects of laser-arc distance on corrosion behavior of single-pass hybrid welded stainless clad steel plate.* Materials & Design, 2017. **123**: p. 80-88.

121. Huang, L., X. Hua, and D. Wu, *Relationship between the weld pool convection and metallurgical and mechanical properties in hybrid welding for butt joint of 10-mm-thick aluminum alloy plate.* Welding in the World, 2018. **62**(5): p. 895-903.

122. Tsukamoto, S., L. Zhao, T. Sugino, and G. Arakane. *Distribution of Wire Feeding Elements in Laser-arc Hybrid Welding.* in *27th International Congress on Applications of Lasers and Electro-Optics (ICALEO).* 2008. Temecula, California, USA: Laser Institute of America.

123. Petring, D., C. Fuhrmann, N. Wolf, and R. Poprawe. *Progress in Laser-MAG Hybrid Welding of High-Strength Steels Up to 30 mm*

Thickness. in *26th International Congress on Applications of Lasers and Electro-Optics (ICALEO)*. 2007. Orlando, Florida, USA: Laser Institute of America.

124. Abt, F., M. Boley, R. Weber, T. Graf, G. Popko, and S. Nau, *Novel X-ray System for in-situ Diagnostics of Laser Based Processes – First Experimental Results.* Physics Procedia, 2011. **12**(Part A): p. 761-770.

125. Matsunawa, A., J.-D. Kim, N. Seto, M. Mizutani, and S. Katayama, *Dynamics of keyhole and molten pool in laser welding* Journal of Laser Applications, 1998. **10**(6): p. 247-254.

126. Zhang, Y., Q. Lin, X. Yin, S. Li, and J. Deng, *Experimental research on the dynamic behaviors of the keyhole and molten pool in laser deep-penetration welding.* Journal of Physics D: Applied Physics, 2018. **51**(14): p. 145602.

127. Wang, H., M. Nakanishi, and Y. Kawahito, *Dynamic balance of heat and mass in high power density laser welding.* Optics Express, 2018. **26**(5): p. 6392-6399.

128. Zhang, M., G. Chen, Y. Zhou, and S. Li, *Direct observation of keyhole characteristics in deep penetration laser welding with a 10 kW fiber laser* Optics Express, 2013. **21**(17): p. 19997-20004.

129. Zhang, L.J., J.X. Zhang, A. Gumenyuk, M. Rethmeier, and S.J. Na, *Numerical simulation of full penetration laser welding of thick steel plate with high power high brightness laser.* Journal of Materials Processing Technology, 2014. **214**(8): p. 1710-1720.

130. Ning, J., L.-J. Zhang, S.-J. Na, X.-Q. Yin, J. Niu, J.-X. Zhang, and H.-R. Wang, *Numerical study of the effect of laser-arc distance on laser energy coupling in pulsed Nd: YAG laser/TIG hybrid welding.* The International Journal of Advanced Manufacturing Technology, 2017. **91**(1): p. 1129-1143.

131. Cho, W.-I., S.-J. Na, M.-H. Cho, and J.-S. Lee, *Numerical study of alloying element distribution in CO2 laser–GMA hybrid welding.* Computational Materials Science, 2010. **49**(4): p. 792-800.

132. Cho, D.-W., W.-I. Cho, and S.-J. Na, *Modeling and simulation of arc: Laser and hybrid welding process.* Journal of Manufacturing Processes, 2014. **16**(1): p. 26-55.

133. Cho, W.-I., S.-J. Na, C. Thomy, and F. Vollertsen, *Numerical simulation of molten pool dynamics in high power disk laser welding.* Journal of Materials Processing Technology, 2012. **212**(1): p. 262-275.

134. Otto, A., and M. Schmidt, *Towards a universal numerical simulation model for laser material processing.* Physics Procedia, 2010. **5**: p. 35-46.

135. Chen, X., S. Pang, X. Shao, C. Wang, J. Xiao, and P. Jiang, *Three-dimensional transient thermoelectric currents in deep penetration laser welding of austenite stainless steel.* Optics and Lasers in Engineering, 2017. **91**: p. 196-205.

136. Otto, A., H. Koch, and R.G. Vazquez, *Multiphysical Simulation of Laser Material Processing.* Physics Procedia, 2012. **39**: p. 843-852.

137. Otto, A., H. Koch, K.-H. Leitz, and M. Schmidt, *Numerical Simulations - A Versatile Approach for Better Understanding Dynamics in Laser Material Processing.* Physics Procedia, 2011. **12**: p. 11-20.

138. Pang, S., X. Chen, J. Zhou, X. Shao, and C. Wang, *3D transient multiphase model for keyhole, vapor plume, and weld pool dynamics in laser welding including the ambient pressure effect.* Optics and Lasers in Engineering, 2015. **74**: p. 47-58.

139. Wu, C.S., H.T. Zhang, and J. Chen, *Numerical simulation of keyhole*

behaviors and fluid dynamics in laser–gas metal arc hybrid welding of ferrite stainless steel plates. Journal of Manufacturing Processes, 2017. **25**: p. 235-245.

140.   Pang, S., X. Chen, W. Li, X. Shao, and S. Gong, *Efficient multiple time scale method for modeling compressible vapor plume dynamics inside transient keyhole during fiber laser welding.* Optics & Laser Technology, 2016. **77**: p. 203-214.

141.   Courtois, M., M. Carin, P. Le Masson, S. Gaied, and M. Balabane, *Guidelines in the experimental validation of a 3D heat and fluid flow model of keyhole laser welding.* Journal of Physics D: Applied Physics, 2016. **49**(15): p. 155503 (13pp).